# Human Motion Reconstruction from Inter-Frame Feature Correspondences of a Single Video Stream Using a Motion Library

Min Je Park[†] Min Gyu Choi[‡] Sung Yong Shin[§]

Computer Science Department
Korea Advanced Institute of Science and Technology [¶]

## Abstract

Videos taken from a single camera are a most common source of human motions. In this paper, we present a novel method to reconstruct the motion of a human-like figure from inter-frame feature correspondences of a single video stream. We exploit a motion library to resolve the depth ambiguity in recovering the 3D configurations from 2D features. Our reconstruction method takes three major steps: timewarping to align the reference motion with that in the video, reconstructing the joint orientations, and estimating the root trajectory. Experimental results show that our approach can reconstruct highly dynamic motions such as shooting of soccer players, which would be hard to do, otherwise.

**CR Categories:** I.3.7 [Computer Graphics]: Three-dimensional Graphics—Animation; G.1.6 [Numerical Analysis]: Optimization

**Keywords:** Computer Animation, Human Motion Reconstruction, Motion Reuse, Nonlinear Optimization

## 1 Introduction

Recently, motion capture techniques have been applied successfully to animating human-like figures. With those techniques, realistic motions can be produced rapidly, which would be hard to achieve, otherwise. Live-captured motion clips are typically short and related to particular characters and environments. Thus, there have been a great deal of efforts to develop specialized tools to reuse them. With the aid of such tools, animators can adapt the captured motions to other characters and environments. However, together with special hardware devices, the motion capture process requires a puppeteer (or an actor) who performs a sequence of motions carefully under a controlled environment in accordance with a scenario. Thus, we cannot directly apply motion capture techniques to reproducing motions in actual situations such as sports events and dance performances.

Monocular videos are a most common source of human motions. Many researchers have tried to capture a variety of human motions from videos for various purposes [1, 2, 3, 12, 13, 17, 20, 23, 24, 26, 29, 30]. However, reconstructing motion from monocular videos is still demanding even with the state of the art techniques. Most of the previous techniques are inadequate to reconstruct highly dynamic motions in a variety of circumstances, and the quality of the reconstructed motion is not adequate to synthesize realistic animation.

To reconstruct human motion from a video, we should recover the 3D configuration of a figure from its 2D features such as the positions of the joints and the end-effectors. The main difficulty in motion reconstruction from a single-camera video stems from the depth ambiguity caused by the 3D projection onto 2D images. Moreover, the focal length of the camera is unavailable, and the camera may move along with the actors. Thus, the actual trajectory of an actor is hard to capture only with the information available in the video.

In this paper, we present a novel method to reconstruct a motion of a human-like figure from a single video stream using a motion library. We assume that the scaled lengths of body segments of an actor in the video and its 2D feature positions are available. Guided by those data, we reconstruct the motion by deforming a captured motion clip in the library. Our approach requires a motion library containing a motion clip similar to the target motion in the video stream. In theory, such a motion library is not always available since human motions are too diverse to be accommodated in the library. We take a practical approach assuming that we know what to reconstruct in advance. For example, suppose that we are to reconstruct shooting motions in a soccer game recorded in a video. After building a library of appropriate live-captured motion clips for shooting, we use them to reconstruct actual players' shooting motions in the video.

## 2 Related Works

### 2.1 Motion Reconstruction

There have been research results [1, 3] to reconstruct human motions from videos automatically with image processing techniques. In those researches, statistical models are employed to estimate 3D configurations of human bodies. Azarbayejani et al. [1] proposed a method to track the motion of a human body with a single/stereo video stream in real-time. They segmented the human body with several blobs and tracked the 3D position of each blob with a statistical dynamic model. Bregler and Malik [3] also estimated the motion from a video sequence taken from one or more cameras. Based on *twist* and *exponential maps* to represent the kinematic relationship of an articulated model, they reconstructed its 3D configuration. Sminchisescu and Triggs [24] pointed out difficulties of optimization for recovering the 3D human body configuration from a single video stream due to the ambiguity and occlusion problems. To possibly avoid local minima, they combined covariance-scaled sampling with numerical optimization.

On the other hand, some researchers have concentrated on de-

[†] email: mjpark@jupiter.kaist.ac.kr
[‡] email: min@jupiter.kaist.ac.kr
[§] email: syshin@jupiter.kaist.ac.kr
[¶] KAIST, 373-1 Kusung-dong Yusung-gu, Taejon, Republic of Korea

veloping efficient ways of extracting 3D information from known 2D features. Zheng and Suezaki [30] introduced a model-based approach to acquire motions of an articulated model from a single video stream. They selected several keyframes to recover the configurations of the model and interpolated them to obtain a motion. Rehg et al. [7] proposed an off-line algorithm to estimate the maximum aposteriori trajectory from the 2D measurements subject to a number of constraints such as a kinematic model and joint angle limits. Barron and Kakadiaris [2] extended this idea to estimate anthropometry measurements from a single video stream. Taylor [26] recovered the 3D configuration of a known articulated structure by considering the foreshortening of the segments of the structure in the image. Liebowitz and Carlsson [16] presented an algorithm for 3D reconstruction of a dynamic articulated structure from uncalibrated multiple views. They exploited constraints associated with the structure, in particular, the conservation of segment lengths over time.

Recently, interesting attempts have been tried to address the reconstruction problem in some different point of view. Howe et al. [12] proposed a scheme to reconstruct the 3D motion of an articulated model from a single video stream. Relying on a priori knowledge about human motion learned from training data, they resolved the inherent depth ambiguity of 2D videos. Sidenbladh et al. [23] also used a learned pattern of walking motion in their Bayesian framework. They treated 3D motion tracking as an inference problem.

To our knowledge, there have not been any methods that can reconstruct, from a single video stream, a highly dynamic motion such as shooting motions in soccer for a full human body consisting of 40 DOFs (degrees of freedom) required for realistic character animation.

### 2.2 Motion Reuse

Due to the success of motion capture technology, there is a vast amount of literature devoted to motion capture and reuse. Bruderlin and Williams [4] introduced the idea of displacement mapping to alter a motion while preserving its details. Witkin and Kass [27] proposed a spacetime constraint technique to produce the optimal motion that satisfies a set of user-specified features. Cohen [5] developed a spacetime control system that allows a user to interactively guide a numerical optimization to find an acceptable solution in a feasible time. Rose et al. [21] adopted this approach to generate a smooth transition between motion clips. Gleicher [10] simplified the spacetime problem by removing the physics-related aspects from the objective function and constraints for motion editing. He also applied this technique for motion retargetting [11]. For interactive performance, Lee and Shin [14] combines a hierarchical curve fitting technique with a new inverse kinematics solver for adaptively refining a motion to meet the spacetime constraints. Popovic and Witkin [18] introduced a novel algorithm that takes dynamics into consideration. They simplified a complex dynamic system without losing the fundamental dynamic properties of motion. Tak et al. [25] proposed a motion balance filter that postprocesses the edited motion to keep the dynamic balance using the notion of a zero moment point (ZMP).

## 3 Overview

In this paper, we introduce a novel method to reconstruct the motion of a human-like figure from a single video stream by using a live-captured motion. We exploit a priori knowledge about the target motion to resolve the depth ambiguity in recovering the 3D configurations from 2D features. We interactively select a motion similar to the target motion from the motion library. Using the motion as a reference, we first warp the reference motion to establish the time correspondence with the motion in the video, and then reconstruct a motion by deforming the timewarped reference motion guided by the features in the video. Since the input video is taken from an uncalibrated camera with an unknown trajectory, we can not directly acquire a root trajectory of the motion from the video. Thus, we first recover the joint orientations to achieve a sequence of postures such that their projected joint positions are coincident with the features in the video. Then, we derive a natural-looking root trajectory, exploiting the set of 2D features derived from kinematic constraints and the dynamic property of the reference motion. Figure 1 shows the block diagram that describes our reconstruction method.

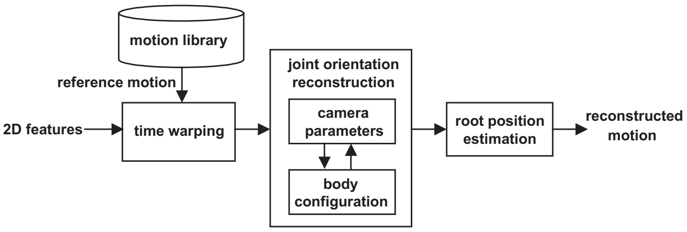

Figure 1: Block diagram of our reconstruction method

To make the time correspondence between the input video and the reference motion, we start with interactively marking their keytimes, that is, the moments of interaction between the actor and his/her surrounding environment in the video. We timewarp the reference motion to synchronize its keytimes with those of the video. This process reparameterizes the reference motion clip. We use the timewarped motion as an initial guess for the target motion.

To obtain a relative posture of the 3D configuration of the articulated figure with respect to the root segment, we establish the constraints that force their projected joint positions to be coincident with the corresponding features in the video. Since there are, in general, multiple configurations that satisfy these constraints, we use an objective function to select a configuration that has minimum deviation from that of the reference motion. We propose an efficient method to acquire the articulated body configuration as well as the unknown camera parameters, simultaneously. To construct a smooth motion, we compute the posture difference between the reference motion and the reconstructed motion at each frame, and then make a posture displacement map that approximates the posture differences with the multilevel B-spline [15]. With this map, we deform the reference motion.

Finally, we estimate a root trajectory to complete the reconstruction process. We have two different cases: In the first case, we deal with the motion that exhibits some interactions between the actor and his/her surrounding environment. In this case, we modify the root trajectory of the reference motion to acquire a feasible root trajectory of the target motion that preserves the interactions. Using the multilevel B-spline approximation technique [15], we interpolate the displacement of the root segment at each frame of the interaction while smoothly propagating approximation errors to neighboring frames. In the second case, we treat a motion that does not show such interactions. In this case, we exploit the dynamic property of the reference motion that should be preserved. In particular, assuming that the articulated figure consists of a set of rigid segments, we obtain the root trajectory of the motion from the center of gravity(COG) trajectory of the reference motion.

The remainder of this paper is organized as follows. Section 4 describes our keytime-based timewarping, and section 5 shows how we can obtain proper camera parameters and a sequence of relative postures from the input video. In section 6, we complete the motion reconstruction process combining the relative postures and the root trajectory. Section 7 demonstrates experimental results for shooting motions of soccer players. After discussing our scheme in section 8, we finally conclude this paper in section 9.

# 4 Timewarping

A motion is a time-varying function that gives the configuration of an articulated figure. For an articulated figure with $n$ joints, we denote a motion by $\mathbf{m}(t) = (\mathbf{p}_1(t), \mathbf{q}_1(t), \cdots, \mathbf{q}_n(t))^T$, where $\mathbf{p}_1(t) \in \mathbb{R}^3$ and $\mathbf{q}_1(t) \in \mathbb{S}^3$ describe the translational and rotational motions of the root segment, respectively, and $\mathbf{q}_i(t) \in \mathbb{S}^3$ give the rotational motion of the $i$-th joint for $2 \leq i \leq n$. We denote the features in a video stream by $\bar{\mathbf{m}}(t) = (\bar{\mathbf{p}}_1(t), \cdots, \bar{\mathbf{p}}_n(t))^T$, where $\bar{\mathbf{p}}(t) \in \mathbb{R}^2$ gives the projected position of the $i$-th joint for $1 \leq i \leq n$. The features given by $\bar{\mathbf{m}}(t)$ represents the projection of the target motion $\mathbf{m}(t)$ onto the image plane at time $t$.

Given the reference motion $\mathbf{m}(t)$ and the 2D features $\bar{\mathbf{m}}(t)$ in the video, we establish a time correspondence between $\mathbf{m}(t)$ and $\bar{\mathbf{m}}(t)$. It is well-known that the dynamic timewarping technique gives an optimal sample correspondences between two functions [4, 6]. However, the camera parameters are not available at each frame. Thus, the dynamic timewarping technique cannot be applied directly to building a time correspondence between $\mathbf{m}(t)$ and $\bar{\mathbf{m}}(t)$, which have different dimensions.

To address this problem, we start with a set of keytimes in the video, that is, the moments of interaction between the actor and his/her surrounding environment. For example, the keytimes of human walking motion can be described as the instances of heel-strikes and toe-offs. For a kick motion in a soccer game, the most important keytime is the impact moment between a foot of a player and a ball. Such a keytime can be easily marked in the video as well as in the reference motion interactively. Assuming that they are available, our task is to timewarp the reference motion to have the same keytimes as specified in the video.

For the $i$-th joint, let $K_i = \{t_{i,1}, \cdots, t_{i,c}\}$ be a set of keytimes for the reference motion and $\bar{K}_i = \{\bar{t}_{i,1}, \cdots, \bar{t}_{i,c}\}$ the counterpart for the video stream. To timewarp the reference motion to make $K_i$ coincide with $\bar{K}_i$ for all $i$, we reparameterize the reference motion $\mathbf{m}(t)$ by a set of linear mappings defined as follows:

$$t^{'}(t) = \bar{t}_{i,k} + \left(\frac{\bar{t}_{i,k+1} - \bar{t}_{i,k}}{t_{i,k+1} - t_{i,k}}\right)(t - t_{i,k}) \ , \qquad (1)$$

where $t_{i,k} \leq t \leq t_{i,k+1}$. Here, $t$ and $t^{'}$ describe the original time of the reference motion and its reparameterized time, respectively. Figure 2 illustrates this procedure for a single joint. Since a human-like articulated figure has multiple joints, we apply this procedure for each joint repeatedly as shown in Figure 3.

# 5 Joint Orientation Reconstruction

## 5.1 Kinematic Constraints

At each frame, the projected joint positions of the articulated figure in the reference motion need to be coincident with their corresponding features in the video. The input video is taken from an uncalibrated camera with unknown trajectory, and the reference objects are not always available in the video. Therefore, to acquire the joint positions in the global frame, we describe them relatively from the root segment. In other words, the configuration of the articulated figure is: $\mathbf{x}(t) = \mathbf{m}(t)|_{\mathbf{p}_1(t)=\mathbf{0}_3}$, that is, $\mathbf{x}(t) = (\mathbf{0}_3, \mathbf{q}(t)_1, \cdots, \mathbf{q}(t)_n)^T$, where $\mathbf{0}_3$ represents the origin of the local frame of the root segment.

To describe the relationship between a 3D configuration of a figure and its projection onto an image plane, we need a camera model. In general, a camera model with full degrees of freedom is parameterized by $\mathbf{c} = (t_x, t_y, t_z, r_x, r_y, r_z, \alpha, f)$, where $(t_x, t_y, t_z)$ and $(r_x, r_y, r_z)$ describes the position and orientation of the camera, respectively, $\alpha$ describes its aspect ratio, and $f$ is its focal length. We assume that the camera aims at the root segment to have its projection placed at the center of the image plane. Then, we can describe the configuration of the camera by the distance to the root of the articulated figure and its orientation. Our reduced camera model is parameterized by $\mathbf{c} = (r_x, r_y, r_z, \gamma)$, where $\gamma$ is the ratio of this distance to $f$. This simple camera configuration is good enough to track the relative motion of each joint with respect to the root position. Later, we will separately estimate the root trajectory to obtain its global motion.

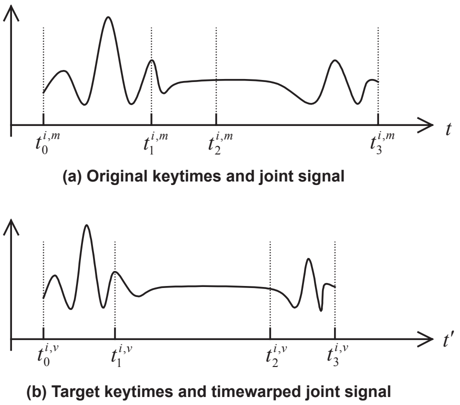

(a) Original keytimes and joint signal

(b) Target keytimes and timewarped joint signal

Figure 2: Timewarping of a reference motion clip using a set of keytimes in the input video sequence and the reference motion. The curve represents the change of one component of a unit quaternion with respect to time. (a) Original joint signal with a set of keytimes, $K_i = \{t_{i,0}, t_{i,1}, t_{i,2}, t_{i,3}\}$. (b) Timewarped motion by a set of keytimes, $\bar{K}_i = \{\bar{t}_{i,0}, \bar{t}_{i,1}, \bar{t}_{i,2}, \bar{t}_{i,3}\}$.

With the camera parameters $\mathbf{c}$, the kinematic constraints on the articulated figure are defined as follows:

$$\|\bar{\mathbf{p}}_i(t) - \mathbf{P}_\mathbf{c}\mathbf{f}_i(\mathbf{x}(t))\| = 0 \qquad (2)$$

where $\mathbf{f}_i(\cdot)$ is the forward kinematic function for the $i$-th joint, and $\mathbf{P}_\mathbf{c}$ describes the projection matrix.

## 5.2 Objective Function

Due to the excessive degrees of freedom for an articulated figure, there are typically many possible configurations that satisfy the kinematic constraints given by Equation 2. DiFranco et al [7] pointed out that this depth ambiguity can be removed partially using some additional constraints such as joint angle limits. Even with such additional constraints, the problem of motion reconstruction is still under-constrained. To achieve the best configuration, we exploit the reference motion for the articulated figure. Assuming that the reference motion is similar to the target motion in the video, the minimum change of the joint orientations from the reference motion ensures the naturalness of the reconstructed motion. Therefore, we find a configuration $\mathbf{x}(t)$ by minimizing the following objective function:

$$g(\mathbf{x}(t)) = dist(\mathbf{x}^r(t), \mathbf{x}(t)). \qquad (3)$$

Here, $\mathbf{x}^r(t)$ describes the configuration of an articulated figure in the reference motion at time $t$, and $dist(\cdot)$ describes the distance between two orientations:

$$dist(\mathbf{x}^r(t), \mathbf{x}(t)) = \sum_{i=1}^{n} \| \ln((\mathbf{q}_i(t))^{-1}\mathbf{q}_i^r(t))\|^2, \qquad (4)$$

where $\ln(\cdot)$ is the logarithmic map of unit quaternions [22].

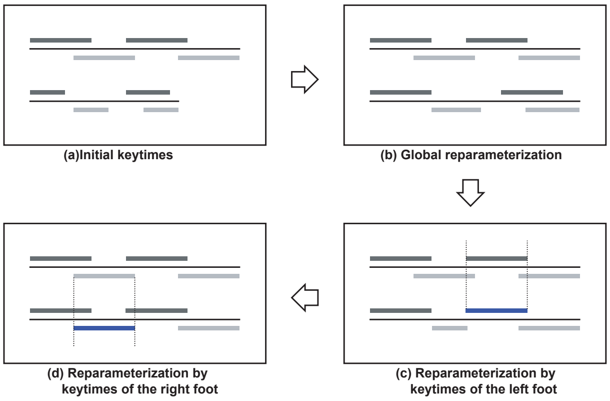
(a)Initial keytimes
(b) Global reparameterization
(d) Reparameterization by keytimes of the right foot
(c) Reparameterization by keytimes of the left foot

Figure 3: Timewarping of a reference motion clip using multiple sets of keytimes in the input video sequence and the reference motion. There are two sets of keytimes for left and right feet. We mark a band between two distinct keytimes for visual aids. (a) Initial sets of keytimes for the left(dark color) and the right(light color) feet in the input video(above) and the reference motion(below) with a time line. (b) Reparameterization of the reference motion to have the same duration with the input video. (c) Reparameterization of the reference motion at a set of keytimes of the left foot. (d) Reparameterization of the reference motion at a set of keytimes of the right foot.

## 5.3 Solution Method

Our joint orientation reconstruction problem is reduced to finding the configuration that minimizes the objective function $g(\cdot)$ while satisfying the constraints given by Equation 2. A typical approach to the constrained optimization is to transform the constrained problem into an unconstrained version with extra penalty functions. The objective function for the unconstrained version is

$$\hat{g}(\mathbf{x}(t)) = \sum_{i=1}^{n}(\|\bar{\mathbf{p}}_i(t) - \mathbf{P_c}\mathbf{f}_i(\mathbf{x}(t))\|^2) + \omega(dist(\mathbf{x}^r(t), \mathbf{x}(t))), \tag{5}$$

where $\omega$ is a weighting factor combing the two different measures. The first term of Equation 5 represents the difference between the projected joint positions of the articulated figure and the marked joint positions in the input video, and the second term measures the deviation of the posture of the figure from that of the reference motion at each time instance. We adopt the conjugate gradient method to minimize this objective function [19].

The major difficulty in solving the Equation 5 stems from the excessive degrees of freedom of an articulated figure. A reasonable human model for computer animation has about 40 degrees of freedom. We have much fewer constraints, compared to the degrees of freedom to determine. Furthermore, the unknown camera parameters complicate the problem. Typical numerical solvers such as conjugate gradient methods show the best convergence property when the objective function has a quadratic form [19]. The Equation 5 is a combined form of parameters for both camera and articulated body configuration. We handle the two different sets of parameters separately during optimization to acquire better convergence. We alternately optimize the camera posture and the body configuration while fixing the other. Figure 4 shows this iterative process of acquiring both camera and body configuration, simultaneously.

It is well-known that a good initial guess for numerical optimization is important to obtain a good solution with better convergence [9, 8, 19]. In our reconstruction method, we use the timewarped reference motion as the initial estimate of the target posture. Since our camera model has four degrees of freedom, we select three coplanar points lying on the center of pelvis and both hip joints of the articulated figure, respectively, to estimate the initial camera configuration with least squares approximation.

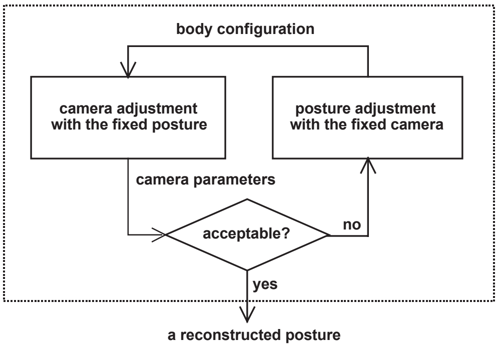
body configuration
camera adjustment with the fixed posture
posture adjustment with the fixed camera
camera parameters
acceptable?
no
yes
a reconstructed posture

Figure 4: Iterative scheme to reconstruct the configuration of the camera and the articulated figure. This procedure starts with an initial configuration of the camera computed by 3 coplanar points specified by a user. The initial guess of the articulated figure is automatically given by the reference motion.

## 5.4 Motion Smoothing

In practice, it is very difficult to track the 2D features in a video precisely without any explicit marker on the human body. Thus, the reconstructed joint orientation contains the jerkiness caused by the noisy 2D features. To reduce such jerkiness, we combine motion displacement mapping [4, 28] with the multilevel B-spline fitting [14, 15]. A motion displacement map describes the difference between two motions. In our case, the displacement map between the configuration of the reference motion $\mathbf{x}^r(t)$ and the recovered configuration $\mathbf{x}(t)$ is defined as $\mathbf{d}(t) = \mathbf{x}(t) \ominus \mathbf{x}^r(t)$, that is,

$$\mathbf{d}(t) = \begin{bmatrix} \mathbf{0}_3 \\ \mathbf{v}_1(t) \\ \vdots \\ \mathbf{v}_n(t) \end{bmatrix} = \begin{bmatrix} \mathbf{0}_3 \\ \mathbf{q}_1(t) \\ \vdots \\ \mathbf{q}_n(t) \end{bmatrix} \ominus \begin{bmatrix} \mathbf{0}_3 \\ \mathbf{q}_1^r(t) \\ \vdots \\ \mathbf{q}_n^r(t) \end{bmatrix} = \begin{bmatrix} \mathbf{0}_3 \\ \ln((\mathbf{q}_1^r(t))^{-1}\mathbf{q}_1(t)) \\ \vdots \\ \ln((\mathbf{q}_n^r(t))^{-1}\mathbf{q}_n(t)) \end{bmatrix}, \tag{6}$$

where $\mathbf{v}_i(t) \in \mathbb{R}^3$ is the rotation vector of the $i$-th joint for $1 \le i \le n$. Thus, a new configuration can be recovered by adding the displacement map to the original motion as $\mathbf{x}(t) = \mathbf{x}^r(t) \oplus \mathbf{d}(t)$, that is,

$$\mathbf{x}(t) = \begin{bmatrix} \mathbf{0}_3 \\ \mathbf{q}_1^r(t) \\ \vdots \\ \mathbf{q}_n^r(t) \end{bmatrix} \oplus \begin{bmatrix} \mathbf{0}_3 \\ \mathbf{v}_1(t) \\ \vdots \\ \mathbf{v}_n(t) \end{bmatrix} = \begin{bmatrix} \mathbf{0}_3 \\ \mathbf{q}_1^r(t)\exp(\mathbf{v}_1(t)) \\ \vdots \\ \mathbf{q}_n^r(t)\exp(\mathbf{v}_n(t)) \end{bmatrix}, \tag{7}$$

From the joint orientation displacement $\mathbf{d}(i)$ at each frame $i$, we compute a smooth displacement map $\mathbf{d}(t)$ that approximates $\mathbf{d}(i)$ for all $i$. We employ the multilevel B-spline approximation technique [15], which uses a series of B-spline functions with different knot spacings on the same interval. In contrast to the local curve fitting with B-splines, the hierarchical structure of the multilevel B-spline fitting can make a smooth shape without undulations, by globally propagating errors at coarse levels and adding details at fine levels. The function from the coarsest knot sequence provides a rough approximation, which is further refined by the functions derived from subsequent finer knot sequences. Finally, we apply the smooth displacement map $\mathbf{d}(t)$ to the reference configuration $\mathbf{x}^r(t)$ to achieve the final configuration $\mathbf{x}^c(t)$ as follows:

$$\mathbf{x}^c(t) = \mathbf{x}^r(t) \oplus \mathbf{d}(t). \tag{8}$$

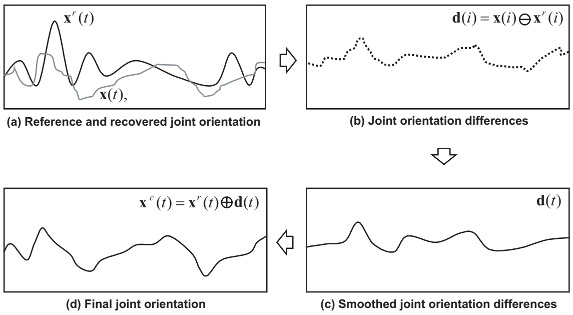

(a) Reference and recovered joint orientation

(b) Joint orientation differences

(d) Final joint orientation

(c) Smoothed joint orientation differences

Figure 5: Smoothing the joint orientation. (a) The curves represent the one component of a unit quaternion of the reference motion and the recovered posture, respectively. (b) Joint orientation differences $\mathbf{d}(i)$. (c) Smoothed joint orientation $\mathbf{d}(t)$ that approximates the differences. (d) Sum of the reference configuration and the smoothed differences.

This procedure is illustrated in Figure 5. Here, we need to trade off the smoothness of the recovered joint orientations against their approximation accuracy, depending on the quality of 2D features. By properly choosing the resolution of knots for noise filtering, we reconstruct a smooth motion even with noisy 2D features while keeping acceptable accuracy.

# 6 Root Position Estimation

In the previous sections, we have described a method to recover the joint orientations of the articulated figure. Now, we construct a proper trajectory of the root segment to complete the reconstruction process. The final motion $\mathbf{m}(t)$ is the direct sum of the joint orientations $\mathbf{x}(t)$ and the displacement map $\mathbf{d}(t)$ that describes only the translational movement of the root segment:

$$\mathbf{m}(t) = \mathbf{x}(t) \oplus \mathbf{d}(t) = \begin{bmatrix} \mathbf{0}_3 \\ \mathbf{q}_1(t) \\ \vdots \\ \mathbf{q}_n(t) \end{bmatrix} \oplus \begin{bmatrix} \mathbf{p}_1(t) \\ \mathbf{0}_3 \\ \vdots \\ \mathbf{0}_3 \end{bmatrix} = \begin{bmatrix} \mathbf{p}_1(t) \\ \mathbf{q}_1(t) \\ \vdots \\ \mathbf{q}_n(t) \end{bmatrix}, \qquad (9)$$

where $\mathbf{p}_1(t)$ is the root trajectory in the global frame. Since the camera may move along with the actors, the actual trajectory of the actor is hard to capture only with the information given in the video. We try to construct a plausible root trajectory while satisfying the user-specified constraints and the dynamic property of the reference motion.

We discriminate two classes of motions according to their interaction with the environment, which is the source of constraints. In the first case, we deal with the motion that exhibits some interaction between the actor and his/her surrounding environment. Locomotion is a typical example since the feet of the actor contact with the ground. In the second case, we treat a motion that does not show such interaction, for which jumping motion is a typical example. In each case, we describe how to obtain the displacement map $\mathbf{d}(t)$, in particular, the root trajectory $\mathbf{p}_1(t)$.

## 6.1 Case 1: Motion involving interaction with the environment

Consider the kick motion of a soccer player as shown in Figure 6. The reconstructed motion is so dynamic that the root trajectory is quite different in height from that of the reference motion. Therefore, we adjust the height of the root segment to make the stance foot contact with the ground at every constrained frame.

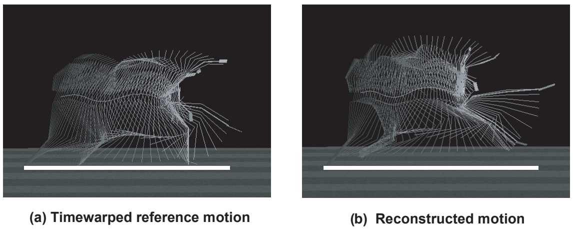

(a) Timewarped reference motion

(b) Reconstructed motion

Figure 6: An artifact of direct substitution of the root trajectory. The artificial ground line is drawn for visual aids. (a) Timewarped reference motion. (b) A motion using the root trajectory of the reference motion. The motion looks like floating above the ground.

We start with the motion $\hat{\mathbf{m}}(t) = \mathbf{x}^c(t) \oplus (\mathbf{p}_1^r(t), \mathbf{0}_3, \cdots, \mathbf{0}_3)^T$, where $\mathbf{x}^c(t)$ and $\mathbf{p}_1^r(t)$ are the recovered joint orientations as explained in Section 5.4 and the root trajectory of the timewarped reference motion, respectively. We compute the distance $\mathbf{d}(i)$ between the stance foot in the motion $\hat{\mathbf{m}}(t)$ and the ground at every constrained frame $i$, and then construct a smooth displacement map $\mathbf{d}(t)$ that approximates $\mathbf{d}(i)$ using the multilevel B-spline approximation method [15]. With $\hat{\mathbf{m}}(t) \oplus (\mathbf{d}(t), \mathbf{0}_3, \cdots, \mathbf{0}_3)^T$ as the initial guess, we adopt the motion retargetting technique [14] to determine the final target motion $\mathbf{m}(t)$.

## 6.2 Case 2: Motion without involving interaction with the environment

Unlike the previous case, a motion in this case does not involve any interaction with the environment as observed in a jump motion. We exploit a dynamics property of the reference motion to determine the root trajectory. Given an initial velocity with no external forces except for gravity, the center of gravity(COG) of an object follows a parabolic trajectory. We measure the initial velocity of the actor at the moment of starting a jump. The COG trajectory $\mathbf{cog}^r(t)$ of the reference motion is defined as follows:

$$\mathbf{cog}^r(t) = \mathbf{p}_1^r(t) + \frac{\sum_{i=1}^n m_i \tilde{\mathbf{p}}_i^r(t)}{\sum_{i=1}^n m_i}, \qquad (10)$$

where $\tilde{\mathbf{p}}_i^r(t)$ and $m_i$ for $1 \le i \le n$ represent the vector from the root position $\mathbf{p}_1^r(t)$ to the COG of the $i$-th link and its corresponding mass, respectively. Since the reference motion is timewarped linearly as described in Section 4, we also linearly scale the COG trajectory of the reference motion to approximate the COG trajectory $\mathbf{cog}(t)$ of the motion to reconstruct as follows:

$$\mathbf{cog}(t) = s\,\mathbf{cog}^r(t) = \mathbf{p}_1(t) + \frac{\sum_{i=1}^n \tilde{\mathbf{p}}_i(t)}{\sum_{i=1}^n m_i}, \qquad (11)$$

where $s$ and $\tilde{\mathbf{p}}_i(t)$ for $1 \le i \le n$ denote the scaling factor for timewarping at the initial frame and the vector from the root position $\mathbf{p}(t)$ to the COG of the $i$-th link, respectively. $\tilde{\mathbf{p}}_i(t)$ can be obtained from the recovered joint orientations $\mathbf{x}^c(t)$. Thus, the root trajectory $\mathbf{p}(t)$ is computed by combining Equations 10 and 11:

$$\mathbf{p}_1(t) = s\mathbf{p}_1^r(t) + s\left(\frac{\sum_{i=1}^n m_i(\tilde{\mathbf{p}}_i^r(t) - \tilde{\mathbf{p}}_i(t))}{\sum_{i=1}^n m_i}\right). \qquad (12)$$

As shown in Figure 7, the reconstructed motion with the root trajectory of the reference motion follows an infeasible, distorted COG trajectory. However, that with the COG trajectory of the reference motion follows a smooth parabolic trajectory.

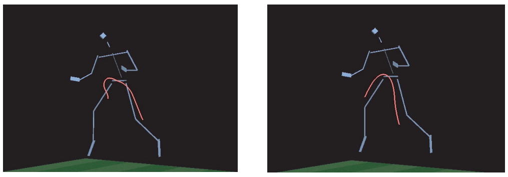

(a) Reconstructed motion with an infeasible COG trajectory (b) Reconstructed motion with an estimated trajectory

Figure 7: Estimating a trajectory of the root segment during a jump motion. The curve represents the COG trajectory of the motion. (a) The reconstructed result using the root trajectory of the reference motion. (b) The reconstructed result using the COG trajectory of the reference motion after timewarping.

# 7 Experimental Results

We use a human model of 40 DOFs: 6 DOFs for the pelvis position and orientation, 3 DOFs for the chest, 3 DOFs for the neck, and 7 DOFs for each limb. The motion clips are sampled at the rate of 60 frames per second, and their keytimes are obtained by interactively specifying the moments of interaction. To demonstrate the effectiveness of our approach in real situations, we recover shooting motions of soccer players from videos. Table 1 shows the repertoire of motion clips in our motion library. All motion clips are captured by an optical motion capture device. Each motion clip contains a highly dynamic motion of a short duration, that is, typically 2∼3 seconds.

We use video clips available on public sites for soccer games. We interactively mark the 2D features in the video, each of which corresponds to a projected joint position of our human model. We also specify the keytimes interactively to build the time correspondence between the reference motion and the video stream.

Our reconstruction method is implemented in C++ on top of MS Windows 2000$^{TM}$ and the TGS Open Inventor$^{TM}$ that is a convenient toolkit to support 3D graphics primitives. Experiments are performed on a Pentium PC (Intel PentiumIII 733MHz processor and 512MB memory).

## 7.1 Kick motion of a soccer player

Figure 8 shows the kick motion of a soccer player we reconstructed with a reference motion clip, “place instep kick”. The video clip used in this example contains 51 frames. The camera tracks the player from the righthand side. There are six keytimes specified in this case: four for the left foot and two for the right foot. Since the target motion takes more inclined postures than the reference motion, the root trajectory has been adjusted to keep the interaction between every stance foot and the ground. Table 2 illustrates the error $e(t)$ of our reconstruction method defined as follows:

$$e(t) = \sum_{i=1}^{n} \|\bar{\mathbf{p}}_i(t) - \mathbf{P_c}\mathbf{f}_i(\mathbf{x}^c(t))\|^2, \tag{13}$$

where $\bar{\mathbf{p}}_i(t)$ and $\mathbf{x}^c(t)$ represent the 2D feature position of $i$-th joint in the image and the final joint configuration at time $t$, respectively. As shown in Table 2, the timewarping reduces the maximum error remarkably. While the unit knot spacing provides a motion that is exactly matched with the features in the video, there exists some jerkiness due to the noisy 2D features. A knot spacing of four gives a smooth motion without significant increase in the average error. It takes 19.34 seconds to reconstruct the kick motion excluding 2D feature marking.

## 7.2 Heading motion of a soccer player

Figure 9 shows the heading motion of a soccer player we reconstructed with a reference motion clip, “left jump heading with both feet”. The video clip used in this example contains 37 frames. In this example, the camera tracks the player from the rear. We specify five keytimes in this case: two for each foot, and one for the head. Since the target motion takes a free flight during the motion with the external force of gravity, the root trajectory has been adjusted to keep the dynamic balance during the jump. The error defined by Equation 13 is shown in Table 2. Excluding the time for 2D feature marking, it takes 14.86 seconds to reconstruct the heading motion.

# 8 Discussion

**Reference Motion Selection:** The availability of a high-quality motion similar to the target motion is the major premise of our method. Suppose that we wish to reconstruct a historical scene such as “Pelle’s shooting” from an old video of a world-cup soccer game. We may collect the data on Pelle’s segment proportions. Provided with a motion library of shooting motions, we bring Pelle’s characteristics into the reference motion to create a Pelle-like shooting motion. Here, we capture Pelle-likeness from the input video and choose the reference motion from the library. At the moment, since the repertoire of such a motion library is rather limited in general, we can select the reference motion interactively by visually examining the motions one by one. We often need to capture additional motions to provide good reference motions. In practice, we are able to reconstruct the target motions successfully from reference motions that look quite different from 2D input motions, as shown in Figures 8 and 9.

**Spacetime Constraints:** The characteristics of the motion such as feature positions at each frame and their inter-frame correspondences are interactively specified. Keytimes are also specified in the same way. If there were any reliable automatic methods, then we would adopt those. The keytimes can be specified easily from the interaction of the body parts with the environment. However, feature tracking is rather challenging since features are often occluded from frame to frame. Fortunately, our scheme does not strictly require every feature position at every frame. In some sense, our reconstruction scheme can be viewed as a spacetime constraint approach for motion synthesis. By marking only the sequence of unoccluded features as spacetime constraints, we construct a displacement map to warp the reference motion while preserving its motion characteristics.

**Motion Synthesis:** We aim at reconstructing human motion from a single video, possibly consisting of uncalibrated images taken at an uncontrolled environment. Therefore, input images inherently have uncertainty hardly resolved by themselves. Moreover, for a video containing highly dynamic motions, inter-frame coherence is too weak to adopt Bayesian framework. To successfully reconstruct a motion in such a situation, we acquire additional helps from a pre-captured motion. Even with a video of a low sampling rate (24Hz) our scheme can produce highly dynamic motion by exploiting a densely-sampled reference motion (60Hz). In this point of view, our scheme can be regarded as a motion synthesis scheme rather than motion reconstruction scheme. In the experiments with 51 frames and 37 frames, respectively, as performed in Section 7, we were able to complete the whole process of each reconstruction in less than 20 minutes including interactive 2D feature marking and keytime specification.

Table 1: Reference motions : kicking and heading motions of soccer players. († represents half-volley) This classification is based on the configuration of legs and heads with respect to ball position.

| category | ball placement | | | | category | head direction | | |
|---|---|---|---|---|---|---|---|---|
| (kicks) | place | volley(h)† | volley | sliding | (headings) | front | left | right |
| instep | ○ | ○ | ○ | - | stand | ○ | ○ | ○ |
| inside | ○ | ○ | - | ○ | jump (single foot) | ○ | ○ | ○ |
| outside | ○ | ○ | ○ | ○ | jump (both feet) | ○ | ○ | ○ |
| toe | ○ | - | - | - | stand back | ○ | ○ | ○ |
| hill | ○ | - | - | - | jump back | ○ | ○ | ○ |
| overhead | - | - | ○ | - | | | | |
| cut | ○ | - | - | - | | | | |
| turning | ○ | - | - | - | | | | |

Table 2: Error analysis data. We compute the minimum, maximum, and average error over all frames. The errors are measured in the normalized coordinate of the image, that is, all the coordinate values are in the interval [-1,1].

| | kick motion (51 frames) | | | heading motion (37 frames) | | |
|---|---|---|---|---|---|---|
| | min. | max. | avg. | min. | max. | avg. |
| original | 0.0331 | 0.3049 | 0.1040 | 0.0116 | 0.1918 | 0.0846 |
| timewarped | 0.0272 | 0.1624 | 0.0915 | 0.0100 | 0.1397 | 0.0710 |
| reconstructed (knot spacing:1) | 0.0011 | 0.0100 | 0.0043 | 0.0005 | 0.0100 | 0.0051 |
| reconstructed (knot spacing:4) | 0.0013 | 0.0227 | 0.0088 | 0.0008 | 0.0159 | 0.0058 |

## 9 Conclusion

In this paper, we have presented a novel method for reconstructing human motions from a single video sequence using a motion library. Our reconstruction method takes three major steps: timewarping to align the reference motion with that in the video, reconstructing the joint orientations, and estimating the root trajectory. Since the motion reconstruction problem is coupled with that of camera posture computation, we also have described a simple camera model to recover the camera configuration from the video sequence for our purpose. Exploiting a 3D motion in the library, we can resolve the inherent depth ambiguities in the reconstruction problem. The reconstructed motion is smooth even with noisy features. Moreover, our method can reconstruct highly dynamic motions, in which the time coherence is weak in the video. Provided with a feasible set of motions as a library, our method can be used to obtain a wide variety of motions in real situations such as sports events. We have demonstrated the effectiveness of our method by reconstructing shooting motions of soccer players from real videos.

## Acknowledgements

We thank Korean Broadcasting System (KBS) for supplying the model in Figures 8 and 9. This research was supported by the National Research Laboratory (NRL) project of Korea Institute of Science & Technology Evaluation and Planning (KISTEP).

## References

[1] A. Azarbayejani, C. Wren, and A. Pentland. Real-time 3-d tracking of the human body. *Proceedings of IMAGE'COM*, May 1996.

[2] C. Barron and I. A. Kakadiaris. Estimating anthropometry and pose from a single image. *In Porc. IEEE Conf. on Computer Vision and Pattern Recognition*, pages 669–676, 2000.

[3] C. Bregler and J.Malik. Estimation and tracking kinematic chains. *In Proc. IEEE Conf. Computer Vision and Pattern Recognition*, 1998.

[4] A. Bruderin and L. Williams. Motion signal processing. *Computer Graphics (Proceedings of SIGGRAPH 95)*, 29(4):97–104, 1995.

[5] M. F. Cohen. Interactive spacetime control for animation. *Computer Graphics (Proceedings of SIGGRAPH 92)*, 26(2):293–302, July 1992.

[6] R. Demori and D. Probst. *Handbook of Pattern Recognition and Image Processing*. Academic Press, 1 edition, 1986.

[7] D.E. Difranco, T.J. Cham, and J.M. Rehg. Recovery of 3d articulated motion from 2d correspondences. *Cambridge Research Laboratory TR-CRL-99-7*, 1999.

[8] R. Fletcher. *Practical Methods of Optimization*. Wiley and Sons, 1 edition, 1980.

[9] P. E. Gill and W. Murray. *Numerical Methods for Constrained Optimization*. Academic Press, 1 edition, 1974.

[10] M. Gleicher. Motion editing with spacetime constraints. *Proc. Symp. Interactive 3D Graphics*, pages 139–148, 1997.

[11] M. Gleicher. Retargetting motion to new characters. *Computer Graphics (Proc. SIGGRAPH '98)*, 32:33–42, July 1998.

[12] N.R. Howe, M.E. Leventon, and W.T. Freeman. Bayesian reconstruction of 3d human motion from single-camera video. *Cambridge Research Laboratory TR-CRL-99-37*, 1999.

[13] I. Kakadiaris and D. Metaxas. Model-based estimation of 3d human motion with occlusion based on active multi-viewpoint selection. *In Proc. IEEE Conf. Computer Vision and Pattern Recognition*, 1996.

[14] J. Lee and S. Y. Shin. A hierarchical approach to interactive motion editing for human-like figures. *Computer Graphics (Proc. SIGGRAPH '99)*, 33:39–48, August 1999.

[15] S. Lee, G. Wolberg, and S. Y. Shin. Scattered data interpolation with multilevel b-splines. *IEEE Trans. Visualization and Computer Graphics*, 3(3):228–244, 1997.

[16] D. Liebowitz and S. Carlsson. Uncalibrated motion capture exploiting articulated structure constraints. *In Proc. 8th International Conference on Computer Vision*, 2001.

[17] T. Noma, K. Oishi, H. Futsuhara, H. Baba, Takeshi Ohashi, and Toshiaki Ejima. Motion generator approach to translating human motion from video to animation. *Pacific Graphics*, October 1999.

[18] Z. Popovic and A. Witkin. Physically-based motion transformation. *Computer Graphics (Proc. SIGGRAPH '99)*, 33:11–20, 1999.

[19] W. H. Press, Saul A. Teukolsky, W. T. Vetterling, and B. P. Flannery. *Numerical Recipes in C: The Art of Scientific Computing*. Cambridge University Press, 2 edition, 1992.

[20] J. M. Rehg and T. Kanade. Visual tracking of high dof articulated structures: an application to human hand tracking. *European Conf. on Computer Vision*, pages 35–46, May 1994.

[21] C. Rose, B. Guenter, B. Bodenheimer, and M. F. Cohen. Efficient generation of motion transitions using spacetime constraints. *Computer Graphics (Proceedings of SIGGRAPH 96)*, 30:147–154, August 1996.

[22] K. Shoemake. Animating rotation with quaternion curves. *Computer Graphics (Proceedings of SIGGRAPH 85)*, 19:245–254, 1985.

[23] H. Sidenbladh, M. J. Black, and D. J. Fleet. Stochastic tracking of 3d human figures using 2d image motion. *European Conference on Computer Vision*, pages 702–718, 2000.

[24] C. Sminchisescu and B. Triggs. Covariance scaled sampling for monocular 3d body trakcing. *In Proc. IEEE Conf. on Computer Vision and Pattern Recognition*, 2001.

[25] S. Tak, O. Song, and H. Ko. Motion balancing filtering. *Computer Graphics Forum*, 19(3):437–446, August 2000.

[26] C. J. Taylor. Reconstruction of articulated objects from point correspondences in a single uncalibrated image. *Computer Vision and Image Understanding*, 80(8):349–363, 2000.

[27] A. Witkin and M. Kass. Spacetime constraints. *Computer Graphics (Proceedings of SIGGRAPH 88)*, 22(4):159–168, August 1988.

[28] A. Witkin and Z. Popovic. Motion warping. *Computer Graphics (Proc. SIGGRAPH '95)*, 29:105–108, August 1995.

[29] C. Wren, A. Azarbayejani, T. Darrell, and A. Pentland. Pfinder: Real-time tracking of the human body. *IEEE Trans. Pattern Analysis and Machine Intelligence*, pages 780–785, July 1991.

[30] J. Y. Zheng and S. Suezaki. A model based approach in extracting and generating human motion. *Proceedings of Fouteenth International Conference on Pattern Recognition*, 2:1201–1205, 1998.

**Human Motion Reconstruction from Inter-Frame Feature Correspondences of a Single Video Stream Using a Motion Library:**
Min Je Park, Min Gyu Choi, and Sung Yong Shin

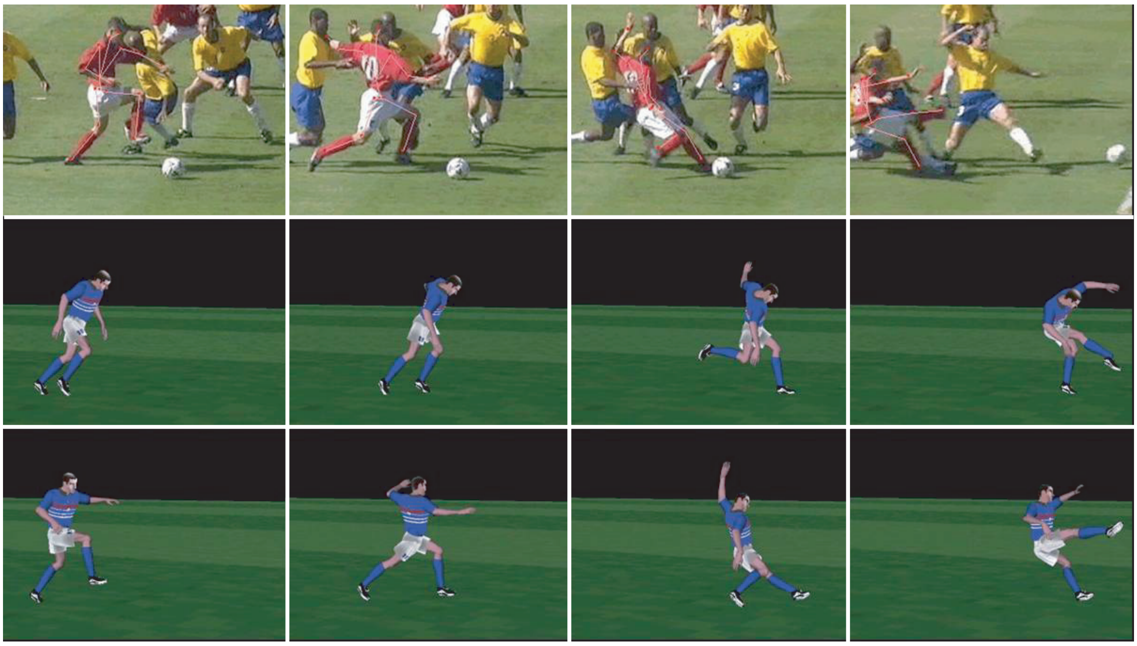

Figure 8: An example with a kick motion. (Top) Input image sequence with feature points. (Middle) Reference motion. (Bottom) Reconstructed motion.

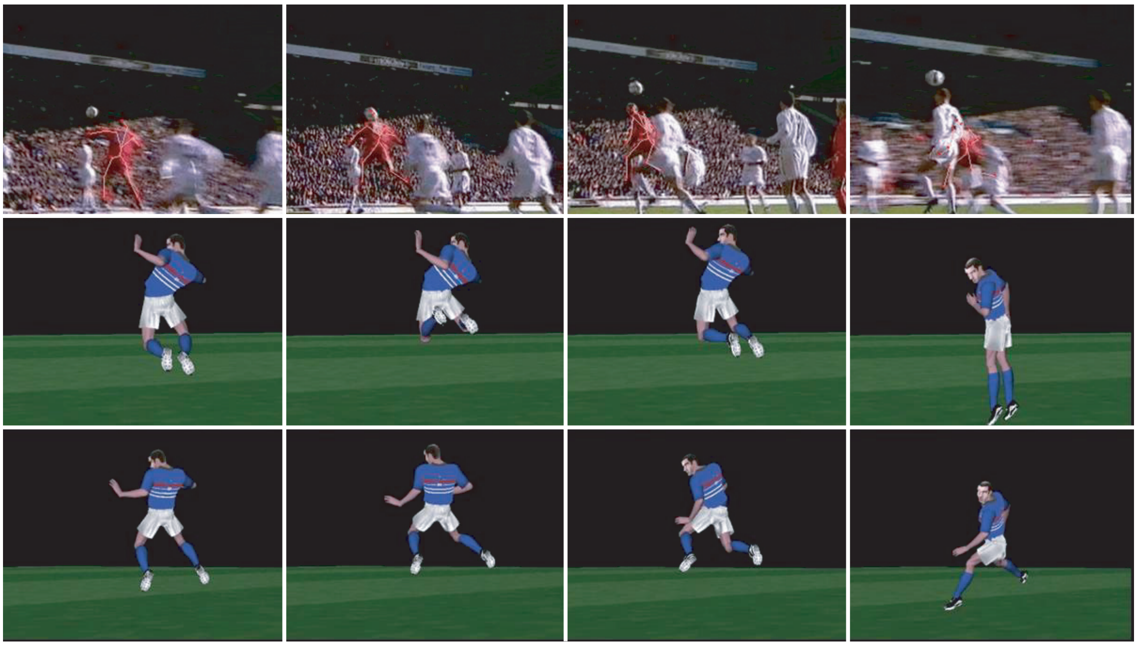

Figure 9: An example with a heading motion. (Top) Input image sequence with feature points. (Middle) Reference motion. (Bottom) Reconstructed motion.